Inorg. Chem. 1988, 27, 3429-3431

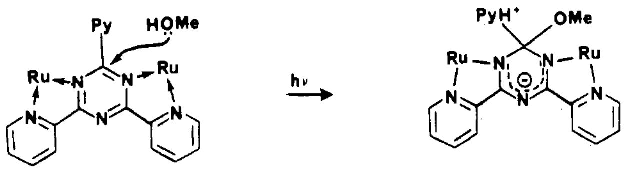

II

Figure 3. Photochemical reaction of MeOH with TPT and $[Ru(CO)_2Cl_2]_n$. The carbonyl and chloride ligands are omitted for clarity.

$O)_2Cl_2L$ (L = 1,10-phenanthroline or 2,2′-bipyridyl) are inert to thermal substitution of CO or X by other ligands.[13] Thus, the formation of a bis-bidentate TPT in I and II is consistent with the unreactive nature of the $Ru(CO)_2Cl_2$ moiety in these compounds.

Spectroscopic data for II are given in the Experimental Section. The IR spectrum contains two strong ν(CO) absorptions in the 1900–2100-cm^{-1} region, indicating cis CO groups. An additional band at 1259 cm^{-1} (which is absent in the spectrum of I) may be assigned to the methoxy C–O–C. The ^1H NMR spectrum of II is very similar to that of I but contains an additional broad peak at δ 8.51, which may be attributed to the H^+ on the uncoordinated pyridyl ring. The recently developed technique of fast atom bombardment (FAB) mass spectrometry has been used to examine nonvolatile complexes,[14] including some ruthenium compounds,[15] and has been used to determine the mass spectrum of II. The mass spectrum shows the $(M - 1)^+$ peak at m/e 801, due possibly to loss of H from the protonated pyridyl ring, and an ion fragment at m/e 770 due to loss of the methoxy group. In addition, ion fragments corresponding to successive loss of CO and Cl are observed at m/e 735 ($(M - MeO - Cl)^+$), 707 ($(M - MeO - Cl - CO)^+$), 672 ($(M - MeO - 2Cl - CO)^+$), and 644 ($(M - MeO - 2Cl - 2CO)^+$). In general, the observed and calculated isotope distributions are in good agreement for most ion fragments.

The electronic spectra of both I and II in the visible region are very similar, with λ_{max} at ca. 420 nm and due most likely to a $d\pi \rightarrow \pi^*$ (TPT) transition. In methanol, yellow solutions of I and II turn green when exposed to light for 15 min. This color change is accompanied by identical changes in the visible spectra of both I and II, i.e. disappearance of the 420-nm band and appearance of two new bands at 382 (ϵ 4.4 × 10^3) and 583 (ϵ 2.8 × 10^3) nm. Irradiation also produces very complex and near-identical NMR patterns for both compounds in DMSO. However, the solution IR spectra (in CH_2Cl_2) of both complexes before and after irradiation remain essentially unchanged in the ν(CO) stretching region (two strong bands at 2066 and 2004 cm^{-1}). Although we have not yet investigated this photochemical reaction in detail, it appears to be reversible since green solutions of I or II, when left in the dark for several hours, revert back to yellow and possess visible and NMR spectral properties almost identical with those of the original solutions prior to irradiation. The fact that the solution IR spectra are unchanged suggests that the reaction does not involve photoisomerization or photolabilization of the cis CO ligands.

Attempts to isolate II by visible irradiation of I in methanol have been unsuccessful, complex I being recovered unchanged. This would suggest that coordination of TPT to ruthenium and methanol addition possibly occur simultaneously, rather than the former preceding the latter. Although free trisubstituted triazines are stable toward nucleophilic hydrolysis,[16] it has been demonstrated that coordination of trisubstituted triazines, such as TPT, assists nucleophilic attack and hydrolysis of the triazine ring.[17] Coordination of two ruthenium ions to TPT would therefore lead to further destabilization of the triazine ring by enhancing its electron deficiency. (In contrast to the case for benzene, triazines are already electron-deficient, as illustrated by their ease of hydrolysis under relatively mild conditions.[18]) This would encourage the addition of methanol, yielding II (Figure 3). Furthermore, the addition of methanol provides some relief to steric hindrance by making the C_3N_3 C(8) tetrahedral.

The only similar substitution reaction involving coordinated TPT reported is the nucleophilic attack at the triazine ring of $[M(TPT)_2]^{2+}$ (M = Ni, Co, Fe, Ru) complexes by hydroxide ions in aqueous solution.[19] However, the substituted complexes were only identified in solution by spectroscopic methods. Furthermore, the photosubstitution by methanol has previously been reported for alkenes and several aromatic and heterocyclic molecules (e.g. ref 20). In view of the current interest in photochemical reactions of ruthenium complexes containing N-heterocyclic ligands, our results would suggest further study of ruthenium–TPT complexes is warranted.

Acknowledgment. This work was partly supported by the AUM Grant-in-Aid program.

Supplementary Material Available: A full table of crystal data and collection parameters and tables of bond distances and angles, anisotropic temperature factors, hydrogen atom coordinates, and least-squares plane calculations (6 pages); a listing of observed and calculated structure factors (27 pages). Ordering information is given on any current masthead page.

---

(13) Kingston, J. V.; Jamieson, J. W. S.; Wilkinson, G. *J. Inorg. Nucl. Chem.* **1967**, *29*, 133.

(14) Bojesen, G. *Org. Mass Spectrom.* **1983**, *20*, 413. Miller, J. M. *Adv. Inorg. Chem. Radiochem.* **1984**, *28*, 2.

(15) Miller, J. M.; Balasanmugam, K.; Nye, J.; Deacon, G. B.; Thomas, N. C. *Inorg. Chem.* **1987**, *26*, 560. Thomas, N. C. *Inorg. Chim. Acta* **1987**, *131*, 151.

(16) Smolin, E. M.; Papport, L. *s-Triazines and Derivatives*; Interscience: New York, **1959**; p 44.

(17) Lerner, E. I.; Lippard, S. J. *Inorg. Chem.* **1977**, *16*, 1546.

(18) Grundman, C.; Kreuterger, A. *J. Am. Chem. Soc.* **1954**, *76*, 5646.

(19) Williams, P. A. *Transition Met. Chem.* **1979**, *4*, 24. Gillard, R. D.; Williams, P. A. *Transition Met. Chem.* **1979**, *4*, 18. Gil, V. M. S.; Gillard, R. D.; Williams, P. A.; Vagg, R. S.; Watton, E. C. *Transition Met. Chem.* **1979**, *4*, 14.

(20) Morrison, H.; Nylund, T. *J. Chem. Soc., Chem. Commun.* **1976**, 785. Nzawa, Y.; Tomioka, H.; Kajami, T.; Sato, T. *J. Chem. Soc., Chem. Commun.* **1977**, 780. Kropp, P. J.; Reardon, E. J.; Gaibel, Z. L. F.; Willard, K. F.; Hattaway, J. H. *J. Am. Chem. Soc.* **1973**, *95*, 7058. Shimazaki, M.; Nakamura, H.; Iitaka, Y.; Ohno, M. *Chem. Pharm. Bull.* **1983**, *31*, 3104.

Contribution from the Nuclear Research Centre Negev,
R. Bloch Coal Research Center, and Chemistry Department,
Ben-Gurion University of the Negev, Beer-Sheva, Israel

Equilibrium Constants for the Homolysis of the Metal–Carbon σ Bond in $[(nta)(H_2O)M^{III}CH_3]^-$ (M = Mn, Fe, Co; nta = Nitrilotriacetate) in Aqueous Solutions

Haim Cohen*,[†] and Dan Meyerstein*,[‡]

Received May 24, 1988

The effect of the nature of the central cation on the stability of metal–carbon σ bonds in a series of analogous complexes is unknown. In a recent pulse radiolysis study[1] we have measured the equilibrium constant, K

$$[(nta)(H_2O)M^{III}CH_3]^- \underset{k_{-1}}{\overset{k_1}{\rightleftharpoons}} [(nta)(H_2O)_2M^{II}]^- + {}^\bullet CH_3 \tag{1}$$

$k_{-1}^{Co} = 1.6 \times 10^8\ M^{-1}\ s^{-1}$ and $K_1^{Co} = 1.4 \times 10^{-8}$ M for M = Co in aqueous solutions (where nta = nitrilotriacetate). It was shown[1] that $[(nta)(H_2O)M^{III}CH_3]^-$, for M = Co, decomposes via homolysis followed by

$$[(nta)(H_2O)M^{III}CH_3]^- + {}^\bullet CH_3 \rightarrow [(nta)(H_2O)M^{II}]^- + C_2H_6 \tag{2}$$

The results indicated also that the technique enables the study of the effect of substituents on the methyl on K_1 and k_2.[1] It was

---

[†] Nuclear Research Centre Negev and R. Bloch Coal Research Center.

[‡] Chemistry Department.

0020-1669/88/1327-3429$01.50/0

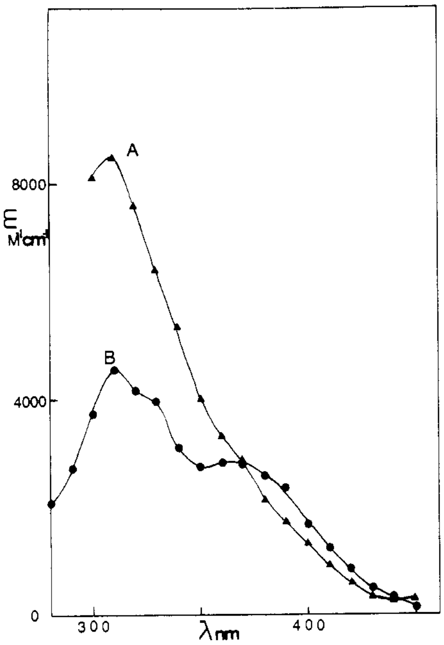

Figure 1. Near-UV spectrum of $[(nta)(H_2O)M^{III}CH_3]^-$ (solution composition of 1×10^{-3} M $M(SO_4)$, 6×10^{-3} M nta, and 0.4 M dimethyl sulfoxide, saturated with N_2O): (A) M = Fe at pH 6.5; (B) M = Mn at pH 6.

shown that K_1 values as high as 1×10^{-2} can be determined.[1] It seemed of interest to try and measure the analogous equilibrium constants for other first-row transition-metal cations and thus study the effect of the nature of the central cation on the stability of metal–carbon σ bonds. In the present study we wish to report K_1 and k_2 for M = Mn and Fe. (For M = Cr,[2] Ni,[3] and Cu[4] different mechanisms of decomposition are observed.)

N_2O-saturated solutions containing $(2-6) \times 10^{-3}$ M nta, $(0.5-5.0) \times 10^{-3}$ M MSO_4 (M = Mn, Fe), and 0.1–0.5 M $(CH_3)_2SO$ in the pH range 4.0–10.5 were irradiated by 0.2–1.5-μs pulses of 200-mA, 5-MeV electrons, from the linear electron accelerator of the Hebrew University of Jerusalem, producing $(0.3-2) \times 10^{-5}$ M free radicals per pulse. All experiments were carried out at room temperature. The experimental setup and data treatment have been described elsewhere in detail.[5] (The iron-containing solutions were prepared in the absence of oxygen by using the syringe technique.)

Under these conditions both e_{aq}^- and $^\bullet OH$ free radicals formed by the pulse[6] are transformed into $^\bullet CH_3$ free radicals via the reaction sequence[7]

$$e_{aq}^- + N_2O \rightarrow {}^\bullet OH + N_2 + OH^- \qquad k = 8.7 \times 10^9\ M^{-1}\ s^{-1} \tag{3}$$

$$^\bullet OH + (CH_3)_2SO \rightarrow (CH_3)_2S(O)OH \qquad k = 7.0 \times 10^9\ M^{-1}\ s^{-1} \tag{4}$$

$$(CH_3)_2S(O)OH \rightarrow CH_3S(O)OH + {}^\bullet CH_3 \qquad k = 1.5 \times 10^7\ s^{-1} \tag{5}$$

When such solutions are irradiated, the formation of short-lived transients with strong absorption bands in the near-UV region is observed (Figure 1). The kinetics of formation and decomposition of these transients were studied. The results point out that the kinetics are independent of $[(CH_3)_2SO]$ and pH in the range 4.0–8.0. The kinetics of the formation of the transients obey a pseudo-first-order rate law, the observed rate depending linearly on $[[(nta)(H_2O)_2M^{II}]^-]$. The straight line describing the dependence on $[[(nta)(H_2O)M^{II}]^-]$, however, does not cross the origin when $[[(nta)(H_2O)_2M^{II}]^-] = 0$ (see for example Figure 2 for M = Fe). The intercept is considerably larger than that which might be attributed to reaction 6, which competes with reaction −1. This

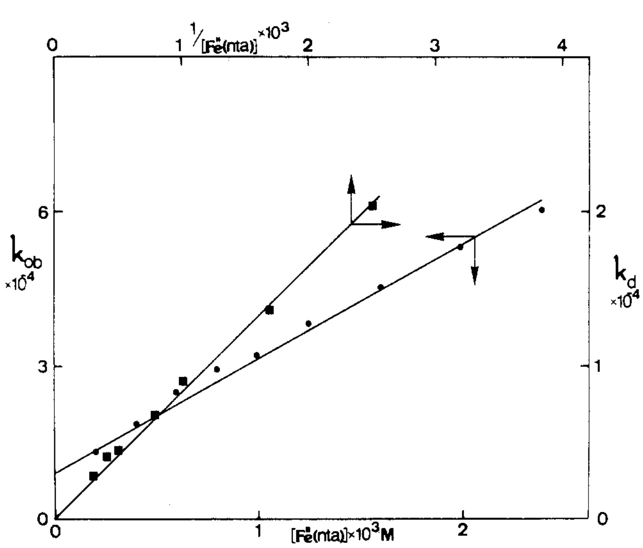

Figure 2. Dependence of the observed rate of formation of $[(nta)(H_2O)Fe^{III}CH_3]^-$, k_{obsd}, on $[[(nta)(H_2O)_2Fe^{II}]^-]$ and the observed rate of decomposition of the transient, k_d, on $1/[[(nta)(H_2O)_2Fe^{II}]^-]$.

$$2^\bullet CH_3 \rightarrow C_2H_6 \qquad k_6 = 1.6 \times 10^9 M^{-1}\ s^{-1} \tag{6}$$

kinetic behavior points out that the reaction of $^\bullet CH_3$ with $[(nta)(H_2O)_2M^{II}]^-$ is indeed an equilibrium reaction, as described by eq 1. k_{-1} is calculated from the slope of the straight line, and k_1 is given by the intercept, after correcting for the contribution of reaction 6. Analysis of the results yields $k_{-1} = (1.48 \pm 0.15) \times 10^8$, $(2.1 \pm 0.3) \times 10^7$ M^{-1}, $k_1 = (1.22 \pm 0.15) \times 10^5$, $(9.0 \pm 2.0) \times 10^3$ s^{-1}, and $K_1 = (8.3 \pm 2.0) \times 10^{-4}$, $(4.3 \pm 1.6) \times 10^{-4}$ M for M = Mn and Fe, respectively. It is of interest to note that for M = Fe an analogous equilibrium reaction with CO_2^- instead of $^\bullet CH_3$ was observed in parallel.[8] The equilibrium constant for the homolysis of $[(nta)(H_2O)Fe^{III}CO_2]^{2-}$ is 1×10^{-5} M.[8]

K_1 can also be calculated from the dependence of the optical density at the end of reaction 1, prior to the decomposition of the short-lived transient, on $[[(nta)(H_2O)_2M^{II}]^-]$. If the equilibrium reaction 1 describes correctly the mechanism, one expects the following dependence of the observed optical density, OD_{obsd}, on the concentration of the divalent complex

$$\frac{1}{OD_{obsd}} = \frac{K_1}{OD^\infty} \frac{1}{[[(nta)(H_2O)_2M^{II}]^-]} + \frac{1}{OD^\infty} \tag{7}$$

where $OD^\infty = C^0 l \epsilon_\lambda([(nta)(H_2O)M^{III}CH_3]^-)$ and $C^0 = [^\bullet CH_3]$ produced by the pulse, l = optical path length, and the absorption due to $^\bullet CH_3$ and $[(nta)(H_2O)_2M^{II}]^-$ at the wavelength of measurement is assumed to be negligible. A plot of $1/OD_{obsd}$ vs $1/[[(nta)(H_2O)_2M^{II}]^-]$ indeed yields straight lines; from the intercept OD^∞ and from the slope K_1 were calculated. The results yield $K_1 = (8.3 \pm 1.7) \times 10^{-4}$, $(5.0 \pm 1.2) \times 10^{-4}$ M, and $\epsilon_{310} = (4.7 \pm 0.5) \times 10^3$, $\epsilon_{350} = (4.6 \pm 0.5) \times 10^3$ M^{-1} cm^{-1} for M = Mn and Fe, respectively. The agreement between the K_1 values thus obtained with those obtained from the kinetic data is very good.

The kinetics of decomposition of the transients obey second-order rate laws. The observed rates (see for example Figure 2) are proportional to $1/[[(nta)(H_2O)_2M^{II}]^-]$ as expected, assuming

---

[1] Meyerstein, D.; Schwartz, H. A. *J. Chem. Soc., Faraday Trans. 1*, in press.

[2] Rotman, A.; Cohen, H.; Meyerstein, D. *Inorg. Chem.* **1985**, *24*, 4158.

[3] Cohen, H.; Meyerstein, D., unpublished results.

[4] Masarwa, M.; Cohen, H.; Meyerstein, D. *Inorg. Chem.* **1986**, *25*, 4897.

[5] Cohen, H.; Meyerstein, D. *Inorg. Chem.* **1974**, *13*, 2434.

[6] Matheson, M. S.; Dorfman, L. M. *Pulse Radiolysis*; MIT Press: Cambridge, MA, 1969; Chapter 6.

[7] Veitwisch, D.; Janata, E.; Asmus, K. D. *J. Chem. Soc., Perkin Trans. 2* **1980**, 146.

[8] Goldstein, S.; Czapski, G.; Cohen, H.; Meyerstein, D. *J. Am. Chem. Soc.* **1988**, *110*, 3903.

that the transients decompose via reaction 2 and not via reaction 6. (In the latter case a linear dependence on $1/[[(nta)(H_2O)_2M^{II}]^-]^2$ is expected.) The observed rate of decomposition, k_d, according to reaction 2 is given by eq 8. k_2 can be

$$k_d = \frac{2k_2K_1}{\epsilon_\lambda([(nta)(H_2O)M^{III}CH_3]^-)\ l}\ \frac{1}{[[(nta)(H_2O)_2M^{II}]^-]} \qquad (8)$$

calculated from the slope of the dependence of k_d on $1/[[(nta)(H_2O)M^{II}]^-]$ and from ϵ_λ and K_1. Thus, $2k_2 = (3.2 \pm 0.6) \times 10^9$ and $(1.1 \pm 0.3) \times 10^9\ M^{-1}\ s^{-1}$ for M = Mn and Fe respectively are obtained. GC analysis points out that indeed over 90% of the $^\bullet CH_3$ free radicals formed by the pulse yield C_2H_6.[9]

The specific rates of reaction of $^\bullet CH_3$ with $[(nta)(H_2O)M^{II}]^-$ are of the same order of magnitude as those reported for the oxidation of the same complexes by Br_2^-, $(NCS)_2^-$, O_2^-, and $^\bullet O_2CH{\cdot}(CH_3)_2OH$.[10] All these reactions occur via the inner-sphere mechanism. It is unclear at present whether reaction 1 follows an S_N1 or an S_N2 mechanism.

The values of $K_1 = 8.3 \times 10^{-4}$, 4.3×10^{-4}, and 1.4×10^{-8} M for M = Mn, Fe, and Co respectively clearly indicate that $\Delta G°$ depends only slightly on the nature of the central cation. One should remember that reaction –1 involves a loss of a water ligand and therefore $\Delta G°$ for the metal–carbon bond dissociation is considerably larger than $\Delta G_1°$. The free energy of reaction 9 is

$$[(nta)(H_2O)_2M^{II}]^- \rightleftharpoons [(nta)(H_2O)M^{II}]^- + H_2O \qquad (9)$$

not known. However, it is reasonable that the effect of the nature of the central cation on $\Delta G_9°$ is analogous to that observed for $\Delta G_{10}°$

$$M(H_2O)_6^{2+} \rightleftharpoons M(H_2O)_5^{2+} + H_2O \qquad (10)$$

i.e. that $\Delta G_9°(Co(II)) > \Delta G_9°(Fe(II)) > \Delta G_9°(Mn(II))$. Thus, it is reasonable to assume that the metal–carbon bond dissociation energy indeed decreases considerably from $Co^{III}–CH_3$ to $Fe^{III}–CH_3$ and $Mn^{III}–CH_3$ as expected.

It is unclear at present whether the $[(nta)(H_2O)M^{III}CH_3]^-$ complexes have a low- or high-spin configuration. The absorption spectrum of the cobalt complex[1] suggests that at least in this case the transient complex has the low-spin configuration.

The role of the ligand nta in enabling the observation of these transients, which are not observed for the analogous aqueous complexes,[11] is not fully understood. Several factors have to be considered:

1. The ligand enhances the rate of the aquo ligand exchange, thus increasing k_{-1}.[13] Only if $k_{-1}[L(H_2O)_nM^{II}][^\bullet CH_3] > k_6[^\bullet CH_3]^2$ is the observation of the transients feasible.
2. The ligand lowers the redox potential of the M(III/II) couple. As reaction –1 is at least formally an oxidation process, it is expected that the stability of the transient will be enhanced by lowering the redox potential of the central cation.
3. The ligand lowers the water–metal bond dissociation energy.

The relative importance of these factors is under study. For this purpose the effect of ligands other than nta on K_1 is being studied.

Finally we would like to point out that reaction 2, which leads to the formation of a carbon–carbon bond, approaches the diffusion-controlled limit in the three systems studied.

Acknowledgment. This study was supported by grants from the Israel Academy of Sciences and Humanities, the Ministry of Energy and Infrastructure and the Planning and Granting Committee of the Council of Higher Education, and the Israel Atomic Energy Commission. D.M. wishes to express his thanks to Irene Evens for her continuous interest and support.

Registry No. $[(nta)(H_2O)Co^{III}CH_3]^-$, 116053-28-2; $[(nta)(H_2O)Mn^{III}CH_3]^-$, 116053-29-3; $[(nta)(H_2O)Fe^{III}CH_3]^-$, 116053-30-6; $[(nta)(H_2O)Co^{II}]^-$, 116053-31-7; $[(nta)(H_2O)Mn^{II}]^-$, 116053-32-8; $[(nta)(H_2O)Fe^{II}]^-$, 116053-33-9; CH_3, 2229-07-4; C_2H_6, 74-84-0.

---

[9] At pH >8.0 the kinetics observed for M = Fe depend on the pH. (These measurements cannot be carried out for M = Mn due to precipitation.) At pH 10.5 $k_{-1} = (5.3 \pm 0.8) \times 10^6\ M^{-1}\ s^{-1}$, $k_1 = (1.05 \pm 0.20) \times 10^3\ s^{-1}$, and $K_1 = (2.0 \pm 1.2) \times 10^{-4}$ M are observed. The results thus suggest that both k_{-1} and k_1 decrease with increasing pH; K_1 seems to decrease slightly, but due to the large error limits this result is not significant. (In the alkaline region the rate of autoxidation of the Fe(II) complex increases and thus the accuracy of the measurements decreases.) The observed rate of decomposition, k_d, decreases by a factor of ca. 30 from pH 8.0 to pH 10.5. This result clearly indicates that k_2 decreases with increasing pH. However, we cannot calculate k_2 accurately in the alkaline region as reaction 6 competes with reaction 2 under the experimental conditions.

[10] Lati, J.; Meyerstein, D. *J. Chem. Soc., Dalton Trans.* **1978**, 1105.

[11] The observation of $(H_2O)_5Fe^{III}CH(CH_3)_2OH^{2+}$ was reported.[12] However, we were unable to reproduce the experimental results.

[12] Pribush, A. G.; Brusenseva, S. A.; Shubin, V. N.; Dolin, P. I. *High Energy Chem.* (*Engl. Transl.*) **1975**, *9*, 206.

[13] Langford, C. H.; Sastri, V. S. In *Reaction Mechanisms in Inorganic Chemistry*; MTP International Review of Science (Inorganic Chemistry, Series One); Butterworths: Oxford, England, 1972; Vol. 9, p 203.

Contribution from the Department of Chemistry,
University of Utah, Salt Lake City, Utah 84112

Preparation and Characterization of Phosphine–Tetraborane(8)

Christopher P. Jock and Goji Kodama*

Received March 24, 1988

Only a few phosphine (PH_3) adducts of boranes have been reported in the literature. Phosphine–borane(3), $BH_3{\cdot}PH_3$, represents a classical example of the compounds. The unique reaction of this adduct with ammonia was first reported by Gamble and Gilmont,[1] and later the reaction and its product were elucidated by Parry and co-workers.[2] The phosphine adduct of triborane(7), $B_3H_7{\cdot}PH_3$, was prepared in this laboratory,[3] and its properties were investigated to compare with those of $BH_3{\cdot}PH_3$. The effect of stronger acidity of the B_3H_7 fragment was apparent: the phosphine hydrogens are more acidic and the B–P bond in $B_3H_7{\cdot}PH_3$ is stronger than those in $BH_3{\cdot}PH_3$.

To further investigate the properties of phosphine adducts of other borane fragments, the next higher borane adduct, $B_4H_8{\cdot}PH_3$, was prepared by cleaving pentaborane(11) (B_5H_{11}) with PH_3. The characterization of $B_4H_8{\cdot}PH_3$ and the formation of a reaction intermediate ($B_5H_{11}{\cdot}PH_3$) are reported in this note.

Results and Discussion

A. Phosphine–Tetraborane(8). When B_5H_{11} and PH_3 were mixed in dichloromethane at –95 °C, a reaction occurred immediately and $B_5H_{11}{\cdot}PH_3$ was formed. At –80 °C in the presence of excess PH_3 a further reaction proceeded, and $B_4H_8{\cdot}PH_3$ and $BH_3{\cdot}PH_3$ were produced. The tetraborane (8) adduct was separated from the reaction mixture as a white solid by evaporating the solvent and then by subliming out $BH_3{\cdot}PH_3$ from the residual solid at –23 °C under vacuum. The compound melted at –6 to –5 °C and decomposed above 0 °C. It was soluble in most organic solvents including dichloromethane, chloroform, diethyl ether, and tetrahydrofuran.

The ^{11}B NMR spectrum of $B_4H_8{\cdot}PH_3$ consists of two sets of resonance signals, α and β, each having the general common pattern of $B_4H_8{\cdot}L$ spectra. (See Figure 1 and Table I.) The presence of the two sets of signals is attributed to two isomeric forms of $B_4H_8{\cdot}PH_3$, endo and exo forms, as many B_4H_8 adducts are known to exist in these two geometrical isomers.[4] The ^{31}P

---

[1] Gamble, E. L.; Gilmont, P. *J. Am. Chem. Soc.* **1940**, *62*, 717.

[2] Gilje, J. W.; Morse, K. W.; Parry, R. W. *Inorg. Chem.* **1967**, *6*, 1761. Dietz, E. A.; Morse, K. W.; Parry, R. W. *Inorg. Chem.* **1976**, *15*, 1.

[3] Bishop, V. L.; Kodama, G. *Inorg. Chem.* **1981**, *20*, 2724.

[4] (a) Centofanti, L. F.; Kodama, G.; Parry, R. W. *Inorg. Chem.* **1969**, *8*, 2072. Paine, R. T.; Parry, R. W. *Inorg. Chem.* **1972**, *11*, 1237. (b) Stampf, E. J.; Garber, A. R.; Odom, J. D.; Ellis, P. D. *Inorg. Chem.* **1975**, *14*, 2446. Odom, J. D.; Moore, T. F.; Dawson, W. H.; Garber, A. R.; Stampf, E. J. *Inorg. Chem.* **1979**, *18*, 2179. Odom, J. D.; Moore, T. F. *Inorg. Chem.* **1980**, *19*, 2651. Odom, J. D.; Zozulin, A. J. *Inorg. Chem.* **1981**, *20*, 3740.

0020-1669/88/1327-3431$01.50/0